

Review

# Can Autism Be Diagnosed with Artificial Intelligence? A Narrative Review

Ahmad Chaddad <sup>1,2,\*</sup> , Jiali Li <sup>1</sup>, Qizong Lu <sup>1</sup>, Yujie Li <sup>1</sup>, Idowu Paul Okuwobi <sup>1</sup>, Camel Tanougast <sup>3</sup> ,  
Christian Desrosiers <sup>2</sup> and Tamim Niazi <sup>4</sup>

<sup>1</sup> School of Artificial Intelligence, Guilin University of Electronic Technology, Guilin 541004, China; indigo.aomg@gmail.com (J.L.); Qizong.lu@hotmail.com (Q.L.); yujieli@guet.edu.cn (Y.L.); paulokuwobi@guet.edu.cn (I.P.O.)

<sup>2</sup> The Laboratory for Imagery, Vision and Artificial Intelligence, École de Technologie Supérieure (ETS), Montreal, QC H3C 1K3, Canada; christian.desrosiers@etsmtl.ca

<sup>3</sup> Laboratoire de Conception, Optimisation et Modélisation des Systèmes, University of Lorraine, 57070 Metz, France; camel.tanougast@univ-lorraine.fr

<sup>4</sup> Lady Davis Institute for Medical Research, McGill University, Montreal, QC H3T 1E2, Canada; tniazi@jgh.mcgill.ca

\* Correspondence: ahmadchaddad@guet.edu.cn

**Abstract:** Radiomics with deep learning models have become popular in computer-aided diagnosis and have outperformed human experts on many clinical tasks. Specifically, radiomic models based on artificial intelligence (AI) are using medical data (i.e., images, molecular data, clinical variables, etc.) for predicting clinical tasks such as autism spectrum disorder (ASD). In this review, we summarized and discussed the radiomic techniques used for ASD analysis. Currently, the limited radiomic work of ASD is related to the variation of morphological features of brain thickness that is different from texture analysis. These techniques are based on imaging shape features that can be used with predictive models for predicting ASD. This review explores the progress of ASD-based radiomics with a brief description of ASD and the current non-invasive technique used to classify between ASD and healthy control (HC) subjects. With AI, new radiomic models using the deep learning techniques will be also described. To consider the texture analysis with deep CNNs, more investigations are suggested to be integrated with additional validation steps on various MRI sites.

**Keywords:** AI; radiomic; autism; deep learning; MRI



**Citation:** Chaddad, A.; Li, J.; Lu, Q.; Li Y.; Okuwobi, I.P.; Tanougast C.; Desrosiers, C.; Niazi, T. Can Autism Be Diagnosed with Artificial Intelligence? A Narrative Review. *Diagnostics* **2021**, *11*, 2032. <https://doi.org/10.3390/diagnostics11112032>

Academic Editor: Kenji Suzuki

Received: 4 October 2021

Accepted: 31 October 2021

Published: 3 November 2021

**Publisher's Note:** MDPI stays neutral with regard to jurisdictional claims in published maps and institutional affiliations.



**Copyright:** © 2021 by the authors. Licensee MDPI, Basel, Switzerland. This article is an open access article distributed under the terms and conditions of the Creative Commons Attribution (CC BY) license (<https://creativecommons.org/licenses/by/4.0/>).

## 1. Introduction

Autism spectrum disorder (ASD) is a pervasive developmental disorder with cognitive abilities that are below normal for their age group. Its core symptoms are categorized by social communication deficits, repetitive stereotypical interests, and persistent patterns of behavior [1]. For example, ASD patients have an inability to understand others' intentions properly, reduced interactive eye contact, etc. Specifically, ASD endangers the physical and mental health of children, placing a burden on patients' social interaction, learning, life, employment, family, and society [2]. In this context, early diagnosis and early intervention for children with ASD can greatly improve the lives of those affected [3]. Unfortunately, ASD has unclear direct indicators and many studies have suggested the genetic factors [4], immunological [5], and neuropsychological associations [6]. The prevalence of mental disabilities among children aged six and below in China is 1/1000, and ASD accounts for 36.9% of them [7]. According to the World Health Organization, the prevalence of ASD is gradually increasing worldwide, with a global average prevalence of 62/10,000 (0.62%), equivalent to one child with ASD in every 160 children. It has become a major global public health problem [8].

Most of the diagnostic tools and methods are based on various tests. The present research on ASD symptoms is not accurate [9]. It is generally believed that children with

ASD will have many problems in their growth and development [10,11]. So far, there are incomplete diagnostic tools for ASD. In this context, a multi assessment is usually considered. ASD could be related to developmental delays and abnormalities. This assessment considers the growth history, parental interview [10], medical examinations, if necessary, and many other things. According to *American Psychiatric Association's Diagnostic and Statistical Manual of Mental Disorders, 5th edition (DSM-5)*, the diagnostic criteria for ASD consist of persistent defects in social communication, social interaction, and restricted and repetitive behavior patterns [11]. In [12], the Autism Diagnostic Observation Schedule (ADOS) is considered the gold standard test because of its reliability, validity, and usefulness. Unfortunately, this test-based screening method can only diagnose children when they have the ability to communicate. We note that there is a great advantage when ASD could be identified at an earlier age. However, according to traditional methods, ASD is difficult to identify at an early age [13] due to the gaps in cognitive abilities in infants at 24 months or older [14]. Even with clinical investigation, deep neurological assessment seems to be more needed. ASD diagnosis is improved by involving many neurological techniques/features (e.g., brain waves [15,16], magnetic resonance images (MRI) [17], and eye-tracking techniques [18], etc.). Another aspect of assessment is related to many genes for predicting ASD [19]. For example, SHANK3 [20] and PTCHD1 [21] are two genes involved in the pathogenesis of ASD through regulation of the nervous system. ITGB3 [22] is associated with the pathogenesis of similar disorders. As with genomic analysis, imaging analysis is a promising technique that leads to identifying ASD patients.

Imaging such as MRI is used to show the anatomy of the brain (e.g., ASD patients) [23]. Two types are the most considered when identifying ASD patients: (1) functional magnetic resonance imaging (fMRI) and (2) structural magnetic resonance imaging (sMRI or MRI) [24]. The fMRI can show brain function, such as active brain regions, while sMRI shows the structure variations (e.g., growth, deformation, atrophy, etc.). In addition, sMRI/MRI is currently the most used technique for imaging the brain structure due to its fast and high-resolution 3D volume imaging. For ASD, sMRI can describe structural brain changes by analyzing gray matter volume, cortical thickness, cortical complexity, and co-variance networks, while fMRI relies on the oxygen content of local tissue vessels (blood oxygen levels depend on functional brain MRI imaging) and can track signal changes in real time. So far, MRI or fMRI provide relevant imaging features that are related to ASD [24].

Imaging features (or radiomics) are widely used in medical image analysis. Among the imaging feature techniques, the following features (radiomics) are the most used for ASD, namely (1) color features, (2) texture, (3) shape/morphology, and (4) spatial relationship features. Briefly, *color features* describe the surface properties of the image. It is not affected by image rotation and translation; *texture features* can better describe the structure image; *shape features* can effectively describe the geometrical area (i.e., region of interest); and *spatial relationship features* can enhance the ability to describe and distinguish the content of the image. These features have been used for many clinical applications such as cancer [25–32], neuroimaging [33,34], segmentation [35], etc. As ASD examples, MRI regional features were computed to study the abnormalities in brain development of ASD patients [36]. In [37], shape features are considered to predict ASD. In [38,39], multiple ASD brain developmental abnormalities are detected during infancy. Moreover, many studies have shown that young children with ASD have a much larger brain size compared to their normally developing peers [40]. The overall volume and density are significantly larger than those of normal children (or healthy control) [41]. Briefly, we will describe the brain differences between ASD and HC as follows:

*Surface area:* Studies have shown that the early cerebral cortex of children with autism expands rapidly between six and twelve months. This atypical expansion leads to problems such as visual receptivity deficits and neglect of social cues [42]. Cortical surface area increases with an accelerated rate between one and two years of age [43]. It coincides with problems of social deficits. Another longitudinal study found that the white matter of the

temporal lobe of the brain increased in autistic children between two and four to five years old. However, the brain grows at a similar rate to normal during this age interval [44]. As a result, the overgrowth of the temporal and frontal lobes is an indicator of ASD [8,43,44].

*Cerebrospinal fluid:* An excessive increase in cerebrospinal fluid can also occur in young children with ASD. During the first few months of life (i.e., within 24 months), infants with ASD have a high volume of inter-axial extra-cerebrospinal fluid [45]. Specifically, the increase in the volume of extra-axial cerebrospinal fluid is more significant at 6 months, which is about 25% higher than ordinary babies. This is related to movement, communication, and the condition of ASD. When the extra-axial cerebrospinal fluid continues to rise, the communication disorder will become more serious [46].

*Structural abnormalities in the white matter:* The corpus callosum develops abnormally at six months. Its area and volume increase significantly [47]. This abnormality is positively correlated with the stereotypical behavior of children with autism [48]. Therefore, structural abnormalities in the white matter are likely to be an important causal factor in the core social deficits (especially emotional disturbances) of later autism.

For ASD diagnosis, clinicians have been committed to using neuroimaging tools. It can automatically distinguish patients with brain diseases from HC or other patients. This can be achieved using features (e.g., imaging, genes, clinical, omics, etc.) with machine learning (ML). ML consists of many methods to classify between classes (e.g., neural networks, support vector machines, random forests, etc.). It learns how to identify the features associated with ASD and then constructs a relevant model. The accuracy of a classifier/predictive model is improved by training the model on large datasets. Eventually, the model can be relied upon to diagnose the presence of ASD. Its accuracy is measured by how well it is able to predict the true class (e.g., ASD). In this context, we aim in this paper to discuss the general radiomics/features and AI/ML model for predicting ASD.

The rest of this paper is structured as follows: Section 2 contains a review of the literature on ASD diagnostic methods. We then discuss the general radiomic methodology for predicting ASD in Section 3. In Section 4, we present the recent explainable artificial intelligence (XAI) literature that is related to ASD. Section 5 discusses the strengths and limitations of ASD predictive models and summarizes the main findings of this study. Last, Section 6 concludes the paper with future recommendations.

## 2. Related Works

Increasing attention has been remarkable for ASD since Leo Kanner talked about it in 1943 and mentioned that it is related to the brain [49–52]. In [49], children with ASD show larger brain volume than HC. In [50], ASD was related to large and small brain white matter hyperplasia and early gray matter hyperplasia, respectively. Compared to HC, ASD children have a larger volume in the amygdala [51] and hippocampus [52,53]. Most of these studies consider the classifications between ASD and HC according to the difference in brain volume or thickness, while texture feature based on gray-scale co-occurrence matrix (GLCM) and Laplacian filter firstly appeared in Chaddad et al. to compare [17] and classify [54] between ASD and HC. As the prevalence of autism increases year by year, effective ASD diagnostic methods have become a major concern worldwide. We summarize three main diagnostic methods as follows:

*Electroencephalography (EEG):* EEG measures neural activity and can detect children at risk of developing ASD and, thus, provide an opportunity for early diagnosis. For example, EEG data is used to compare between ASD and HC [16,55,56]. In [57], the CNN model was used for classification after converting the data into 2D form. Although EEG can be used to diagnose ASD, it still has limitations in a number of conditions (e.g., signal noises).

*Eye tracking:* It is based on characteristic changes of eyes, such as periphery and iris. In [58], they studied 86 two-year-old's (26 ASD, 38 HC, and 22 developmentally delayed children). It shows that eyes with ASD were associated with passive insensitivity to social signals. In [59], they selected 29 ASD children aged between 5 and 11 years. Through the visualization of real faces and avatars, it was possible to study how children

with ASD recognize emotions. For ASD patients, eye tracking is not an optimal method because it takes a long time for children to cooperate. In addition, it is not flexible for clinical diagnosis.

*MRI/fMRI scans:* Data quality of MR imaging is improving in function with the advanced technology. Previous studies have shown that brain structures in patients with ASD can differ significantly in terms of volume, thickness, and texture [54,60]. However, this scenario is still under radiomic and AI investigation for ASD diagnosis. Yet, no clear tools have been involved in the clinical system. However, we find many works prove that classifier models using extracted features from MRI/fMRI images have the ability to predict ASD patients. For example, a support vector machine (SVM) model has shown an accuracy value of 66.8% to predict ASD images [24]. In [61], 12 classifiers are compared, namely six nonlinear shallow ML models, three linear shallow models, and three deep learning models. A dense feedforward network provides the best results among the 12 models with an AUC value of 80%. This demonstrates that even when using features derived from imaging data, deep learning methods, such as the dense feedforward network, can provide higher predictive accuracy over classical ML methods [61]. To let the AI models be feasible for ASD prediction, more investigation is recommended since the performance metrics are still limited. In addition, no clear study is considered when the images from an MRI scanner consist of 7 Tesla or above. We believe that more resolution of images will let the radiomic with texture analysis be more informative for predicting ASD [17,54].

### 3. Radiomic Methodology

To provide a wider perspective to the readers, the radiomic pipeline is simply given in Figure 1. It illustrates the processing steps for the radiomic pipeline that consist of image acquisition and preprocessing, segmentation, feature extraction, statistical analysis, and classifications. We describe, below, a detailed review of each step.

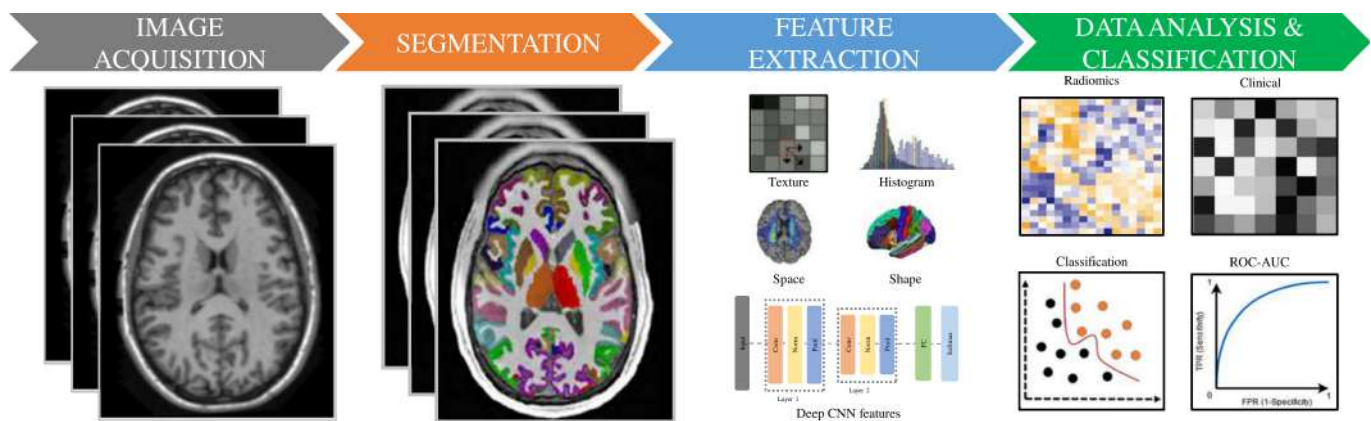


**Figure 1.** General radiomic workflow for predicting ASD. Schematic illustration of the entire radiomic process, including image acquisition with preprocessing with symptomatic ASD patients undergoing MR (MRI and/or fMRI) scans. After image segmentation, radiomic features are extracted and selected. Data aggregation for statistical modeling, with classifier modeling employed for classifying ASD from HC.

#### 3.1. Image Acquisition and Preprocessing

The purpose of preprocessing is to improve the visual effect of the image. It can purposely emphasize the overall or partial characteristics of the image for various scenarios [62]. For example, it can improve the color, brightness, and contrast of the image. There are two main methods for image enhancement: (a) Spatial domain, which includes image gray-scale transformation, histogram correction [63], local statistics method, image smoothing, and image sharpening, etc. As in [64], fast non-rigid registration can improve the contrast of the brain structures. In [65], the image enhancement method is based on brightness level and gradient modulation. This method reduces the dynamic range of the brightness level and enhances the details (i.e., texture) of the image. (b) Frequency domain,

which transforms an image into the frequency domain for filtering using Fourier analysis. The image is then inversely transformed back into the spatial domain. The most used frequency-domain methods are the homomorphic filtering [66] and wavelet transform [67]. Therefore, image denoising plays a major role for texture analysis. It can be described by probability distribution function and probability density function. We note that the texture analysis could be related to the scale of image filtering and then to ASD [68].

### 3.2. Normalization/Standardization

Image normalization is one of the preprocessing steps to avoid image distortions (i.e., translation, rotation, scaling, and skew). However, the main challenge for ASD studies is related to MRI images derived from multisites [69–71]. For example, scans from multisites lead to high differences of texture features between these sites. In [72], min–max normalization is used to overcome the image variation and convert the image values to a range of [0–1]. Normalization of images here improves the learning rate, reduces the dependence on initialization, and reduces the training time to overcome the overfitting problem. In [73], non-parametric models are used to correct intensity inhomogeneities and avoid the scanner distortions. In [74], MRI was normalized using voxel-based morphometry (VBM) that is available in the Statistical Parametric Mapping software (<https://www.fil.ion.ucl.ac.uk/spm/software/>, accessed on 19 September 2021). VBM technique is spatially normalizing the MRI scans to the same stereotactic space to correct nonuniform intensity variations [75]. Recent work shows that domain adaptation can effectively reduce the site variation using the CNN models [71], (e.g., Table 1). However, more work on image normalization for multisite variation is needed to extract the texture features for radiomic analysis.

**Table 1.** Summary of ASD studies using MRI/fMRI with machine learning models.

Work	Data Source	Cases Number	Data Type	FEM	Classifier Model	Acc	Sen	Spec	AUC
[76]	FSL	50 ASD and 50 HC	TfMRI	SPF	DWT-CNN	80%	84%	76%	-
[77]	ABIDE-I+II	23 ASD and 15 HC	Rs-fMRI	SPF	SVM	80.76%	-	-	-
[78]	NDAR	185 subjects	sMRI-fMRI	SF	RF	80.8%	84.9%	79.2%	81.92%
[79]	ABIDE	505 ASD and 530 HC	Rs-fMRI	SPF	Ridge Return	71.98%	-	-	-
[80]	ABIDE	518 ASD and 567 HC	rs-fMRI	SF	CNN	71.8%	81.25%	68.75%	67%
[81]	Private	40 ASD and 36 HC	MRI	SF	SVM	84.2%	80%	88.9%	-
[82]	ABIDE-I	505 ASD and 530 HC	rs-fMRI	OF	DNN	70%	74%	63%	-
[24]	ADHD-200	279 ASD and 279 HC	fMRI	TF	SVM	64.91%	44.16%	81.91%	-
[83]	ABIDE-I+II	76 ASD and 75 HC	MRI	TF and SF	SVM	64.3%	77%	82%	69%
[84]	ABIDE-I	155 ASD and 186 HC	T1-MRI	SF	HGNN	76.7%	-	-	-
[85]	ABIDE-I+II	255 ASD and 276 HC	rs-fMRI	SF	SVM	75.00–5.23%	90.62%	90.58%	-
[86]	ABIDE	539 ASD and 573 HC	T1-MRI	SF	6 classifiers	>80%	-	-	-
[87]	ABIDE	539 ASD and 573 HC	rs-fMRI	OF	SVM	86.7%	87.5%	85.7%	-
[88]	ABIDE	99 ASD and 85 HC	fMRI	SPF	CNN	68.54%	69.49%	67.58%	-
[89]	ABIDE-I	270 ASD and 305 HC	rs-fMRI	SPF	ANN	74.54%	63.46%	84.33%	-
[90]	ABIDE-I	48 ASD and 24HC	MRI	TF and SF	RF	98%	-	-	52.5–53%
[91]	ABIDE	49 ASD and 41 HC	rs-fMRI	SF	SVM	78.89%	85.71%	70.73%	-
[92]	ABIDE	539 ASD and 573 HC	fMRI	SF	CNN	87%	-	-	-
[93]	ABIDE-I	505 ASD and 530 HC	fMRI	SF	CNN	70.22%	77.46%	61.82%	74.86%
[72]	ABIDE-I	79 ASD and 105 HC	3D-fMRI	OF	CNN	94.7%	-	-	94.703%
[85]	ABIDE-I+II	255 ASD and 276 HC	rs-fMRI	SF	SVM-RFECV	75.0–95.23%	90.62%	90.58%	-
[94]	ABIDE-I	368 ASD and 449 HC	sMRI	SF	AE, MLP	85.06%	-	-	-
[95]	ABIDE-I+II	620 ASD and 542 HC	rs-fMRI	SF	3D-CNN,SVM	72.3%	-	-	-
[96]	ABIDE-I	505 ASD and 530 HC	rs-fMRI	OF	CNN	82.69%	88.23%	88.67%	-

Table 1. Cont.

Work	Data Source	Cases Number	Data Type	FEM	Classifier Model	Acc	Sen	Spec	AUC
[97]	ABIDE-I	403 ASD and 468 HC	fMRI	OF	SVM	76.8%	72.5%	79.9%	81%
[98]	ABIDE-II	26 ASD and 26 HC	MRI	SF	SVM-RFE	73%	71%	75%	81%
[99]	ABIDE-I	403 ASD and 468 HC	rs-fMRI	SF	RNN-LSTM	74.74%	72.95%	-	-
[100]	ABIDE-I	505 ASD and 530 HC	fMRI	SF	SAE	70.8%	62.2%	79.1%	-
[101]	ABIDE-I	505 ASD and 530 HC	sMRI	SF	RFE+RF	72%	-	-	-
[94]	ABIDE-I	368 ASD and 449 HC	sMRI	SF	AE	85.06 ± 3.52%	-	-	-
[102]	NDAR	47 ASD and 24 HC	rs-fMRI	OF	SVM-RFE	86%	81%	88%	-
[103]	ABIDE	539 ASD and 573 HC	fMRI	SF	RCE-SVM	70.01%	-	-	-
[87]	ABIDE-I	539 ASD and 573 HC	rs-fMRI	SF	SVM	86.7%	87.5%	85.7%	-
[104]	NDAR	33 ASD and 33 HC	fMRI	SF	1D-CNN	77.2%	78.1%	76.5%	-
[105]	ABIDE	41 ASD and 41 HC	rs-fMRI	OF	KNN	85.9%	79.3%	92.6%	-

SPF: spatial feature, TF: texture features, SF: shape/morphological feature, OF: other features, rs-fMRI: resting state-functional magnetic resonance imaging, T1-MRI: T1-weighted magnetic resonance imaging, ABIDE I and II: autism brain imaging data exchange I and II, NDAR: National Database for Autism Research, FSL: fMRI software library, SVM-RFECV: support vector machine-recursive feature elimination with a stratified-4-fold cross validation, AE: autoencoder, SAE: stacked autoencoder, DWT-CNN: discrete wavelet transform-convolutional neural network, MLP: multi-layer perceptron, DNN: deep neural networks, KNN: Kohonen neural network, RNN: recurrent neural networks, LSTM: long short-term memory, SVM-RFE: support vector machines-recursive feature elimination, RCE-SVM: recursive cluster elimination-support vector machines, FEM: feature extraction method, Acc: accuracy, Sen: sensitivity, Spec: specificity, AUC: area under curve, HGNN: hypergraph neural network, +: combination, >: is greater than, ±: plus or minus.

### 3.3. Segmentation/Labeling

ASD segmentation aims to label the brain regions (e.g., region of interest). An image is divided into several regions with similar properties. Currently, clustering and deep learning techniques are the main methods for segmenting brain MRI images [106]. For example, deep learning is able to properly segment the corpus callosum (CC) [107]. This technique reduces the need for manual or semi-automatic segmentation of neuroanatomical. Manual and semiautomatic segmentation can be performed on a brain MRI using the 3D Slicer tool [108]. However, deep learning-based segmentation offered significant algorithms for labeling brain regions in an automatic fashion [109]. Actually, the most used tool for ASD image preprocessing, standardization, and brain region labeling is the FreeSurfer [110]. Specifically, it processes the 3D structure brain image, and performs automatic cortical and subcortical labeling. By generating accurate gray and white matter, and cerebrospinal fluid regions, it can compute cortical thickness and other surface characteristics. Specifically, for ASD, FreeSurfer is widely used in the preprocessing of MRI images. For example, it is used to preprocess and extract features from MRI images of ASD patients [78]. While it is analyzed, high-quality MRI images in [111]. It is also considered when generating brain morphological features, including regional volume, surface area, average cortical thickness, and Gaussian curvature [112].

### 3.4. Features Extraction

An image consists of many features that define the behavior of an image [113]. Specifically, feature extraction techniques aim to find the most important information to save computational work and data storage. Briefly, we summarize three types of image features that are used for predicting ASD: (1) shape features, (2) spatial features, and (3) texture features.

*Shape features:* This type of feature is related to the geometric and morphological region of interest (e.g., brain subcortical regions). For example, many studies consider the shape features to predict ASD patients [50–52]. The shape feature problem is represented by unreliable results when the target is deformed, in addition to distortion due to changes in viewpoint. We note that Hough transform and Fourier shape descriptors are classical methods to extract shape features. Despite the wide use of shape features, this type of feature does not describe the content of the image. Then, in combination with other informative features, it may improve performance metrics [17,54].

*Spatial features:* It refers to the spatial position or relative direction. It can strengthen the description and distinction of image content, while the rotation and change of the scale can affect the spatial characteristics. There are two ways to extract the spatial relationship: (1) extract the features using the automatic segmentation (objects, colors, etc.) and (2) by generating an index. Alternatively, you can segment the image uniformly, extract the features from each image separately, and consider the index. Furthermore, spatial features have advantages in diagnosing ASD patients of different ages and genders. For example, spatial filter can provide highly discriminative features between ASD patients and neurotypical subjects [114]. However, there are few studies that used spatial features for ASD diagnosis due to the constraint of high-dimensional data and a relatively small dataset [115].

*Texture feature:* Most of the current literature for predicting ASD based on images is based on shape features. However, the potential of MRI images has not been fully developed. Fortunately, studies such as [17,54] have proved that texture features can classify patients with ASD. Specifically, texture features reflect the homogeneity of the image [17,54]. These features describe the surface properties of the image [116]. Specifically, the texture is based on a statistical order that is widely used for many topics. For example, gray-level co-occurrence matrix (GLCM) is currently one of the best statistical techniques for computing image texture. Computation of GLCM reflects comprehensive information about the direction, adjacent interval, and gray level of an image. In addition, the local patterns and their arrangement rules are analyzed using this technique.

### 3.5. Feature Selection

Due to the high-dimensional nature of MRI data, features may consist of redundant information [87]. Feature selection is a procedure to choose the dominant features. Specifically, feature selection algorithms aim to find the most predictive features by removing irrelevant or redundant features. This procedure improves the classifier model performance and reduces the running time [117]. These algorithms can be classified to three methods, namely filter, wrapper, and embedded [118,119].

*Filter method (FM):* The features of each dimension are given weights which represent the importance of the feature. These features are then ranked according to the weights [120]. A number of features are selected using a threshold. The typical methods are Pearson correlation coefficient and Chi-square test. This kind of feature selection algorithm has low algorithmic complexity and is suitable for large-scale datasets. However, it has a lower classification performance compared to wrapper algorithms.

*Wrapper method (WM):* It divides the features into different combinations, evaluates the combinations, and compares them with other combinations. Typical methods are represented by recursive feature elimination (REF), stepwise selection, backward elimination, etc. These algorithms are convenient with some studies. Despite the advantage of wrapper methods, more investigations to generalize these algorithms are needed [121].

*Embedded method (EM):* The feature selection algorithm itself is embedded in the learning algorithm as a component [118]. ML models are used for training, then obtain the weight coefficients of each feature. Features are selected based on coefficients from the largest to smallest (similar to the filter method, except that the coefficients are trained). This method is considered an efficient technique to select predictive features.

Table 2 reports the techniques used recently for feature selection in ASD studies. For example, wrapper methods are generally used more compared to filtering and embedding. As expected, the predictive feature derived WM is considered higher performance than FM [122]. Due to the difficulty of setting parameters, the use of EM is limited. More details about feature selection techniques are reported in [123].

### 3.6. Statistical Analysis and Classification Models

To predict the ASD images, features extracted are used as input to a classifier model. Many ML models could be used as predictive models. The ML models are generally

divided into two types: supervised and unsupervised [124]. An algorithm based on supervised learning uses labeled input and output data, while an unsupervised learning algorithm does not. We summarize two groups of ML methods: conventional methods (i.e., SVM, KNN, RF, etc.) and deep learning (e.g., CNN, RNN, LSTM, etc.).

**Table 2.** Summary of feature selection techniques related to ASD.

Work	Feature Group	Feature Selection Type	Technique
[81]	SF	WM	Identify the feature group that achieves the best performance through greedy forward feature selection.
[87]	OF	WM	A feature selection algorithm based on a minimum spanning tree is proposed to find the optimal feature set.
[101]	SF	WM	Use recursion to perform feature selection.
[125]	OF	FM	Use Pearson correlation coefficient to filter redundant features.
[126]	OF	WM	Use recursive feature elimination (RFE) to rank the importance of features and then remove irrelevant features recursively.
[127]	OF	WM	Use the reverse order feature selection algorithm.
[128]	OF	WM	Adopt a restricted path depth-first search algorithm (RP-DFS).
[129]	OF	FM	Chi-square is used to remove non-significant features.
[91]	SF	EM	Use principal component analysis (PCA) to select the principal components.
[130]	SF	EM	Use the sure independence screening (SIS) method. Multiple features are removed in each iteration.

SF: shape/morphological feature, OF: other features, FM: filter method, WM: wrapper method, EM: embedded method

Table 1 reports the performance metrics in predicting ASD using the current feature extraction techniques and various image sources (ABIDE ([http://fcon\\_1000.projects.nitrc.org](http://fcon_1000.projects.nitrc.org), accessed on 19 September 2021), NDAR (<https://nda.nih.gov>, accessed on 19 September 2021) and FSL (<https://www.fmrib.ox.ac.uk/datasets/>, accessed on 19 September 2021)). We found that shape/morphological and texture features generally lead to a higher accuracy rate compared to shape or texture features. We noted that the use of texture features is still limited due to the limited resolution of MRI/fMRI scans with 1.5 or 3 Tesla. Thus, more investigation related to texture analysis is recommended for improving the performance metrics.

*Conventional method:* The most popular is the SVM. It is in many neuroimaging tasks [81,131,132]. However, SVM is not recommended when the samples are less than the features number due to the overfitting. In this context, random forest can solve this problem by automatically selecting the features to build the classifier model [133]. RF combines random feature selection and bootstrap aggregation to build a collection of decision trees that exhibit controlled variation [134]. To tune the parameters of conventional models, a grid search on a validation set is considered. In addition, many types of validation steps such as cross validation are used to test the classifier model [135].

*Deep learning:* Deep learning is a part of ML models, advanced with new hardware technology such as a graphics processing unit (GPU). Recently, deep learning demonstrated remarkable classification results in clinical applications [136]. In [88], a hybrid model consisting of CNN with brain features was used to improve the performance metrics. In addition, some literature combined conventional methods and deep learning to improve the performance and overcome overfitting [95].

*Statistical and performance metrics:* For evaluating the classifier models, many performance metrics are considered. However, the common measurements are the area under the receiver operating characteristic (ROC) curves (AUC), accuracy, sensitivity, and specificity. To compare between classes (e.g., ASD versus HC), significance tests are used to measure the  $p$  value. Correction of significant values (e.g.,  $p < 0.05$ ) is recommended following the Holm–Bonferroni correction (or using other correction techniques) [137]. For example, we note that the range value of classification accuracy is 70.01–94.7% and depends on the features extracted, classifier model, and data source (see Table 1). We observed that the most common models are CNNs and SVMs. However, CNN demonstrates higher performance



metrics compared to other models [138]. Moreover, ML or deep learning algorithms require a large dataset to generalize a reliable predictive model, which is not currently available in a medical field. To obtain benefit from deep learning, a transfer learning technique is used to overcome the overfitting and time computation [139]. Although, for the potential of deep learning for clinical tasks, more work is required to understand the mechanism of such algorithms (e.g., information flow of CNN for classifications [140]).

#### 4. Explainable Artificial Intelligence

Recent literature for reporting clinical research involving deep learning will realize the full potential of machine learning tools [141,142]. Unfortunately, these models (i.e., algorithms) work as a black box in the medical field [143]. It is not explained how to correlate inputs and outputs or the mechanism of information flow in the hidden layers [144]. XAI provides interpretability for algorithms, models, and tools. It aims to make AI algorithms more transparent to improve human understanding of these models. For example, CNNs can automatically extract features based on their convolutional layers and its interpretability is crucial for personalized diagnosis (e.g., ASD [145], Coronavirus [146], etc.). The output can be mapped back to the input space to see which parts of the input are discriminative [147]. In [148], loss function is considered for each filter within the high-level convolutional layer to produce interpretable activation patterns. In [149], convolutional layers of CNN models are quantified to understand the information flow from input to output of architecture for predicting Alzheimer disease using MRI images. EEG data were used to detect emotions in ASD patients, and an interpretable deep learning technique (SincNet) was investigated [150]. In addition, an explainable SVM model for ASD identification was studied by demonstrating a link between the dominant features and the model outcome [151].

Applying such XAI models in predicting ASD images will provide more details about the brain subcortical regions related to ASD. Most of the XAI is focused on model-agnostic post-hoc explainability algorithms due to their easier integration and wider reach [152]. Interpretable AI techniques can be generally characterized from a different perspective [153]. While the former strategies are easier to grasp and hence adopt, their effectiveness is often limited, necessitating the deployment of more sophisticated procedures. Deep radiomic analysis, in which the CNN layers are encoded and utilized as input into a classifier model, is one of the most active study areas in XAI [34,146,149]. In this context, deep radiomic analysis seeks to provide high-level transparency of deep learning algorithms in the health data (e.g., images). Despite XAI gaining traction, evaluating these methods is still a challenge and poses an open question in the future of XAI research in clinical tasks.

#### 5. Discussion

Using radiomics with AI models is considered a pioneering development of precision medicine work [149,154] such as in mental disorders (e.g., ASD) [155]. This is motivating to make a systematic overview of the radiomic application for ASD diagnosis. There are only two classes (ASD and HC) available in the public domain, which are not able to investigate all subtypes of ASD. Although fMRI and sMRI data are publicly available in the ABIDE dataset, the results of combining these multisite data for ASD diagnosis using radiomics and deep learning models have not yet been investigated. As we previously mentioned, the texture features depend on the MRI sites that led to bias when we combined all ABIDE sites. Nowadays, assistive tools using domain adaptation algorithms can reduce this issue; however, the problems still dominate when implementing these algorithms in real-world scenarios.

This study demonstrated the various uses of radiomic models in diagnosing and classifying ASD, along with their strengths and limitations. Critical examples of radiomic pipelines for ASD with classification accuracy, different evaluation measures, and essential feature selection, and their techniques and dataset sources, have been discussed and analyzed. However, certain prevailing problems need to be addressed, such as learning

from limited data, considering inappropriate sampling methods, classification between imbalanced datasets, and how we involve the XAI in radiomic analysis. Integrating AI in clinical settings would not only improve our knowledge of ASD but will also allow healthcare practitioners to employ these methods as clinical decision support systems for screening and diagnostic processes. To sum up, we summarize the main findings of this study on ASD as follows:

- MRI-based models for the diagnosis of ASD are more suitable for clinical trials than eye tracking and CT image analysis. MRI can provide more detail of the brain.
- The brain of ASD patients can be heterogeneous in many locations (e.g., hippocampus, amygdala, etc.). The variation could be captured by shape features (e.g., volume, thickness, etc.).
- Deep learning is still challenging to diagnose ASD patients due to the lack of benchmark datasets [156].
- XAI could be the solution as a diagnostic model for ASD. However, it needs more investigation in real-world scenarios.
- The public dataset needs to be continually expanded to avoid inappropriate studies due to insufficient data. In addition, it needs to be ensured that there is no error in results due to age, gender, etc. [157].

## 6. Conclusions

In this paper, we present a survey of AI related to ASD using MRI/fMRI scans. We discussed the general radiomic features and classifier models that are used for predicting the ASD images. Recent studies show that the texture features are informative features. Among the deep learning models, CNN demonstrates the highest metrics. However, more investigation is needed in the context of XAI. For future work, high-precision and high-transparency models can be established by quantifying the deep texture from CNN models to predict early ASD patients.

**Author Contributions:** Conceptualization, A.C.; methodology, A.C., J.L. and Q.L.; writing—original draft preparation, A.C., J.L. and Q.L.; writing—review and editing, A.C., I.P.O., C.D., C.T., Y.L. and T.N.; project administration, A.C.; All authors have read and agreed to the published version of the manuscript.

**Funding:** This research received no external funding.

**Institutional Review Board Statement:** Not applicable.

**Informed Consent Statement:** Not applicable.

**Conflicts of Interest:** The authors declare no conflict of interest.

## References

1. Hyman, S.L.; Levy, S.E.; Myers, S.M. Identification, evaluation, and management of children with autism spectrum disorder. *Pediatrics* **2020**, *145*, e20193447. [[CrossRef](#)] [[PubMed](#)]
2. van't Hof, M.; Tisseur, C.; van Berckeleer-Onnes, I.; van Nieuwenhuyzen, A.; Daniels, A.M.; Deen, M.; Hoek, H.W.; Ester, W.A. Age at autism spectrum disorder diagnosis: A systematic review and meta-analysis from 2012 to 2019. *Autism* **2021**, *25*, 862–873. [[CrossRef](#)] [[PubMed](#)]
3. Tao, L. Research Progress on Early Recognition of Childhood Autism Spectrum Disorder. *China Matern. Child Health Care* **2020**, *35*, 1554–1558.
4. Toma, C. Genetic variation across phenotypic severity of autism. *Trends Genet.* **2020**, *36*, 228–231. [[CrossRef](#)] [[PubMed](#)]
5. Al-Ameen, S.A.; Tawfeeq, F.K.; Shihab, K.A. Estimation of Some Biochemical and Immunological Parameters of Autism Spectrum Disorder. *Biochem. Cell. Arch.* **2020**, *20*, 1601–1604.
6. Haigh, S.M.; Keller, T.A.; Minshew, N.J.; Eack, S.M. Reduced white matter integrity and deficits in neuropsychological functioning in adults with autism spectrum disorder. *Autism Res.* **2020**, *13*, 702–714. [[CrossRef](#)] [[PubMed](#)]
7. Center, W.C.B.M. *China Autism Education and Rehabilitation Industry Development Report*; Beijing Normal University Press: Beijing, China, 2015.
8. Lord, C. The future of autism: Global & local achievements & challenges. *Indian J. Med. Res.* **2020**, *151*, 263.

9. Kim, S.H.; Bal, V.H.; Benrey, N.; Choi, Y.B.; Guthrie, W.; Colombi, C.; Lord, C. Variability in autism symptom trajectories using repeated observations from 14 to 36 months of age. *J. Am. Acad. Child Adolesc. Psychiatry* **2018**, *57*, 837–848. [[CrossRef](#)]
10. Crowell, J.A.; Keluskar, J.; Gorecki, A. Parenting behavior and the development of children with autism spectrum disorder. *Compr. Psychiatry* **2019**, *90*, 21–29. [[CrossRef](#)]
11. Arbanas, G. Diagnostic and Statistical Manual of Mental Disorders (DSM-5). *Codas* **2015**, *51*, 61–64.
12. Lord, C.; Risi, S.; Lambrecht, L.; Cook, E.H.; Leventhal, B.L.; DiLavore, P.C.; Pickles, A.; Rutter, M. The Autism Diagnostic Observation Schedule—Generic: A standard measure of social and communication deficits associated with the spectrum of autism. *J. Autism Dev. Disord.* **2000**, *30*, 205–223. [[CrossRef](#)] [[PubMed](#)]
13. Farooq, A.; Ahmed, S. Sociocultural Barriers to Early Diagnosis of Autism Spectrum Disorder. *Life Sci.* **2020**, *1*, 6. [[CrossRef](#)]
14. Miller, L.E.; Dai, Y.G.; Fein, D.A.; Robins, D.L. Characteristics of toddlers with early versus later diagnosis of autism spectrum disorder. *Autism* **2021**, *25*, 416–428. [[CrossRef](#)] [[PubMed](#)]
15. Jayawardana, Y.; Jaime, M.; Jayarathna, S. Analysis of temporal relationships between ASD and brain activity through EEG and machine learning. In Proceedings of the 2019 IEEE 20th International Conference on Information Reuse and Integration for Data Science (IRI), Los Angeles, CA, USA, 30 June–1 August 2019; pp. 151–158.
16. Heunis, T.; Aldrich, C.; Peters, J.; Jeste, S.; Sahin, M.; Scheffer, C.; De Vries, P. Recurrence quantification analysis of resting state EEG signals in autism spectrum disorder—A systematic methodological exploration of technical and demographic confounders in the search for biomarkers. *BMC Med.* **2018**, *16*, 101. [[CrossRef](#)]
17. Chaddad, A.; Desrosiers, C.; Toews, M. Multi-scale radiomic analysis of sub-cortical regions in MRI related to autism, gender and age. *Sci. Rep.* **2017**, *7*, 45639. [[CrossRef](#)]
18. Vacas, J.; Antolí, A.; Sánchez-Raya, A.; Pérez-Dueñas, C. Eye Tracking Methodology for Studying Emotional Competence in Children with Autism Spectrum Disorder (ASD) and Specific Language Impairment (SLI): A Comparative Research Review. *Rev. J. Autism Dev. Disord.* **2021**, *5*, 1–15.
19. Cederquist, G.Y.; Tchieu, J.; Callahan, S.J.; Ramnarine, K.; Ryan, S.; Zhang, C.; Rittenhouse, C.; Zeltner, N.; Chung, S.Y.; Zhou, T. A multiplex human pluripotent stem cell platform defines molecular and functional subclasses of autism-related genes. *Cell Stem Cell* **2020**, *27*, 35–49. [[CrossRef](#)]
20. Soorya, L.; Kolevzon, A.; Zweifach, J.; Lim, T.; Dobry, Y.; Schwartz, L.; Frank, Y.; Wang, A.T.; Cai, G.; Parkhomenko, E. Prospective investigation of autism and genotype-phenotype correlations in 22q13 deletion syndrome and SHANK3 deficiency. *Mol. Autism* **2013**, *4*, 1–17. [[CrossRef](#)]
21. Noor, A.; Whibley, A.; Marshall, C.R.; Gianakopoulos, P.J.; Piton, A.; Carson, A.R.; Orlic-Milacic, M.; Lionel, A.C.; Sato, D.; Pinto, D. Disruption at the PTCHD1 Locus on Xp22. 11 in Autism spectrum disorder and intellectual disability. *Sci. Transl. Med.* **2010**, *2*, 49ra68. [[CrossRef](#)]
22. Napolioni, V.; Lombardi, F.; Sacco, R.; Curatolo, P.; Manzi, B.; Alessandrelli, R.; Militerni, R.; Bravaccio, C.; Lenti, C.; Saccani, M. Family-based association study of ITGB3 in autism spectrum disorder and its endophenotypes. *Eur. J. Hum. Genet.* **2011**, *19*, 353–359. [[CrossRef](#)]
23. Nordahl, C.W.; Mello, M.; Shen, A.M.; Shen, M.D.; Vismara, L.A.; Li, D.; Harrington, K.; Tanase, C.; Goodlin-Jones, B.; Rogers, S. Methods for acquiring MRI data in children with autism spectrum disorder and intellectual impairment without the use of sedation. *J. Neurodev. Disord.* **2016**, *8*, 1–10. [[CrossRef](#)] [[PubMed](#)]
24. Sen, B.; Borle, N.C.; Greiner, R.; Brown, M.R. A general prediction model for the detection of ADHD and Autism using structural and functional MRI. *PLoS ONE* **2018**, *13*, e0194856. [[CrossRef](#)]
25. Chaddad, A.; Kucharczyk, M.J.; Daniel, P.; Sabri, S.; Jean-Claude, B.J.; Niazi, T.; Abdulkarim, B. Radiomics in glioblastoma: Current status and challenges facing clinical implementation. *Front. Oncol.* **2019**, *9*, 374. [[CrossRef](#)]
26. Chaddad, A.; Daniel, P.; Desrosiers, C.; Toews, M.; Abdulkarim, B. Novel radiomic features based on joint intensity matrices for predicting glioblastoma patient survival time. *IEEE J. BioMed Health Inform.* **2018**, *23*, 795–804. [[CrossRef](#)] [[PubMed](#)]
27. Chaddad, A.; Daniel, P.; Niazi, T. Radiomics evaluation of histological heterogeneity using multiscale textures derived from 3D wavelet transformation of multispectral images. *Front. Oncol.* **2018**, *8*, 96. [[CrossRef](#)]
28. Chaddad, A.; Desrosiers, C.; Toews, M. Radiomic analysis of multi-contrast brain MRI for the prediction of survival in patients with glioblastoma multiforme. In Proceedings of the 2016 38th Annual International Conference of the IEEE Engineering in Medicine and Biology Society (EMBC), Orlando, FL, USA, 16–20 August 2016; pp. 4035–4038. [[CrossRef](#)]
29. Chaddad, A.; Zinn, P.O.; Colen, R.R. Brain tumor identification using Gaussian Mixture Model features and Decision Trees classifier. In Proceedings of the 2014 48th Annual Conference on Information Sciences and Systems (CISS), Princeton, NJ, USA, 19–21 March 2014; pp. 1–4.
30. Chaddad, A.; Daniel, P.; Sabri, S.; Desrosiers, C.; Abdulkarim, B. Integration of radiomic and multi-omic analyses predicts survival of newly diagnosed IDH1 wild-type glioblastoma. *Cancers* **2019**, *11*, 1148. [[CrossRef](#)] [[PubMed](#)]
31. Chaddad, A.; Desrosiers, C.; Abdulkarim, B.; Niazi, T. Predicting the Gene Status and Survival Outcome of Lower Grade Glioma Patients With Multimodal MRI Features. *IEEE Access* **2019**, *7*, 75976–75984. [[CrossRef](#)]
32. Chaddad, A.; Desrosiers, C.; Toews, M.; Abdulkarim, B. Predicting survival time of lung cancer patients using radiomic analysis. *Oncotarget* **2017**, *8*, 104393. [[CrossRef](#)]

33. Zhang, M.; Zhang, F.; Zhang, J.; Chaddad, A.; Guo, F.; Zhang, W.; Zhang, J.; Evans, A. AutoEncoder for Neuroimage. In Proceedings of the International Conference on Database and Expert Systems Applications, Linz, Austria, 27–30 September 2021; pp. 84–90.
34. Chaddad, A.; Desrosiers, C.; Niazi, T. Deep radiomic analysis of MRI related to Alzheimer’s disease. *IEEE Access* **2018**, *6*, 58213–58221. [[CrossRef](#)]
35. Chaddad, A.; Tanougast, C. Quantitative evaluation of robust skull stripping and tumor detection applied to axial MR images. *Brain Inform.* **2016**, *3*, 53–61. [[CrossRef](#)]
36. Yang, L.; Zhu, Z.; Cao, M.; Liu, B.; Guo, J.; Wan, G. SMRI study of early brain overdevelopment in children with autism. *Magn. Reson. Imaging* **2020**, *11*, 264–269.
37. Xiuyan, W. Prediction Research on Autism Based on Structural Magnetic Resonance Imaging. Ph.D. Thesis, Beijing Jiaotong University, Beijing, China, 2018.
38. Smith, E.; Thurm, A.; Greenstein, D.; Farmer, C.; Swedo, S.; Giedd, J.; Raznahan, A. Cortical thickness change in autism during early childhood. *Hum. Brain Mapp.* **2016**, *37*, 2616–2629. [[CrossRef](#)] [[PubMed](#)]
39. Wolff, J.J.; Jacob, S.; Elison, J.T. The journey to autism: Insights from neuroimaging studies of infants and toddlers. *Dev. Psychopathol.* **2018**, *30*, 479–495. [[CrossRef](#)]
40. Lainhart, J.E.; Piven, J.; Wzorek, M.; Landa, R.; Santangelo, S.L.; Coon, H.; Folstein, S.E. Macrocephaly in children and adults with autism. *J. Am. Acad. Child Adolesc. Psychiatry* **1997**, *36*, 282–290. [[CrossRef](#)] [[PubMed](#)]
41. Sacco, R.; Gabriele, S.; Persico, A.M. Head circumference and brain size in autism spectrum disorder: A systematic review and meta-analysis. *Psychiatry Res. Neuroimaging* **2015**, *234*, 239–251. [[CrossRef](#)] [[PubMed](#)]
42. Elison, J.T.; Paterson, S.J.; Wolff, J.J.; Reznick, J.S.; Sasson, N.J.; Gu, H.; Botteron, K.N.; Dager, S.R.; Estes, A.M.; Evans, A.C. White matter microstructure and atypical visual orienting in 7-month-olds at risk for autism. *Am. J. Psychiatry* **2013**, *170*, 899–908. [[CrossRef](#)]
43. Hazlett, H.C.; Gu, H.; Munsell, B.C.; Kim, S.H.; Styner, M.; Wolff, J.J.; Elison, J.T.; Swanson, M.R.; Zhu, H.; Botteron, K.N. Early brain development in infants at high risk for autism spectrum disorder. *Nature* **2017**, *542*, 348–351. [[CrossRef](#)]
44. Nassar, N.; Dixon, G.; Bourke, J.; Bower, C.; Glasson, E.; De Klerk, N.; Leonard, H. Autism spectrum disorders in young children: Effect of changes in diagnostic practices. *Int. J. Epidemiol.* **2009**, *38*, 1245–1254. [[CrossRef](#)] [[PubMed](#)]
45. Wang, R. Morphological Brain Network Research on Childhood Autism. Ph.D. Thesis, University of Electronic Science and Technology of China, Chengdu, China.
46. Shen, M.D.; Kim, S.H.; McKinstry, R.C.; Gu, H.; Hazlett, H.C.; Nordahl, C.W.; Emerson, R.W.; Shaw, D.; Elison, J.T.; Swanson, M.R.; et al. Increased extra-axial cerebrospinal fluid in high-risk infants who later develop autism. *Biol. Psychiatry* **2017**, *82*, 186–193. [[CrossRef](#)]
47. Wolff, J.J.; Gerig, G.; Lewis, J.D.; Soda, T.; Styner, M.A.; Vachet, C.; Botteron, K.N.; Elison, J.T.; Dager, S.R.; Estes, A.M. Altered corpus callosum morphology associated with autism over the first 2 years of life. *Brain* **2015**, *138*, 2046–2058. [[CrossRef](#)]
48. Wolff, J.J.; Swanson, M.R.; Elison, J.T.; Gerig, G.; Pruett, J.R.; Styner, M.A.; Vachet, C.; Botteron, K.N.; Dager, S.R.; Estes, A.M. Neural circuitry at age 6 months associated with later repetitive behavior and sensory responsiveness in autism. *Mol. Autism* **2017**, *8*, 1–12. [[CrossRef](#)] [[PubMed](#)]
49. Piven, J.; Saliba, K.; Bailey, J.; Arndt, S. An MRI study of autism: The cerebellum revisited. *Neurology* **1997**, *49*, 546–551. [[CrossRef](#)]
50. Courchesne, E.; Karns, C.; Davis, H.; Ziccardi, R.; Carper, R.; Tigue, Z.; Chisum, H.; Moses, P.; Pierce, K.; Lord, C. Unusual brain growth patterns in early life in patients with autistic disorder: An MRI study. *Neurology* **2001**, *57*, 245–254. [[CrossRef](#)]
51. Nordahl, C.W.; Iosif, A.M.; Young, G.S.; Hechtman, A.; Heath, B.; Lee, J.K.; Libero, L.; Reinhardt, V.P.; Winder-Patel, B.; Amaral, D.G.; et al. High Psychopathology Subgroup in Young Children With Autism: Associations With Biological Sex and Amygdala Volume. *J. Am. Acad. Child Adolesc. Psychiatry* **2020**, *59*, 1353–1363.e2. [[CrossRef](#)]
52. Reinhardt, V.P.; Iosif, A.M.; Libero, L.; Heath, B.; Rogers, S.J.; Ferrer, E.; Nordahl, C.; Ghetti, S.; Amaral, D.; Solomon, M. Understanding hippocampal development in young children with autism spectrum disorder. *J. Am. Acad. Child Adolesc. Psychiatry* **2020**, *59*, 1069–1079. [[CrossRef](#)]
53. Li, G.; Chen, M.H.; Li, G.; Wu, D.; Sun, Q.; Shen, D.; Wang, L. A Preliminary Volumetric Mri Study of Amygdala and Hippocampal Subfields in Autism During Infancy. *IEEE Int. Symp. Biomed. Imaging* **2019**, *2019*, 1052–1056.
54. Chaddad, A.; Desrosiers, C.; Hassan, L.; Tanougast, C. Hippocampus and amygdala radiomic biomarkers for the study of autism spectrum disorder. *BMC Neurosci.* **2017**, *18*, 52. [[CrossRef](#)] [[PubMed](#)]
55. Bosl, W.J.; Tager-Flusberg, H.; Nelson, C.A. EEG analytics for early detection of autism spectrum disorder: A data-driven approach. *Sci. Rep.* **2018**, *8*, 1–20. [[CrossRef](#)]
56. Vicnesh, J.; Wei, J.K.E.; Oh, S.L.; Arunkumar, N.; Abdulhay, E.; Ciaccio, E.J.; Acharya, U.R. Autism spectrum disorder diagnostic system using HOS bispectrum with EEG signals. *Int. J. Environ. Res. Public Health* **2020**, *17*, 971.
57. Peya, Z.J.; Akhand, M.; Srabonee, J.F.; Siddique, N. EEG Based Autism Detection Using CNN Through Correlation Based Transformation of Channels’ Data. In Proceedings of the 2020 IEEE Region 10 Symposium (TENSYP), Dhaka, Bangladesh, 5–7 June 2020; pp. 1278–1281.
58. Moriuchi, J.M.; Klin, A.; Jones, W. Mechanisms of diminished attention to eyes in autism. *Am. J. Psychiatry* **2017**, *174*, 26–35. [[CrossRef](#)] [[PubMed](#)]

59. Pino, M.C.; Vagnetti, R.; Valenti, M.; Mazza, M. Comparing virtual vs. real faces expressing emotions in children with autism: An eye-tracking study. *Educ. Inf. Technol.* **2021**, 1–16. [[CrossRef](#)]
60. Albajara Sáenz, A.; Van Schuerbeek, P.; Baijot, S.; Septier, M.; Deconinck, N.; Defresne, P.; Delvenne, V.; Passeri, G.; Raeymaekers, H.; Slama, H. Disorder-specific brain volumetric abnormalities in attention-deficit/hyperactivity disorder relative to autism spectrum disorder. *PLoS ONE* **2020**, *15*, e0241856. [[CrossRef](#)]
61. Mellema, C.; Treacher, A.; Nguyen, K.; Montillo, A. Multiple Deep Learning Architectures Achieve Superior Performance Diagnosing Autism Spectrum Disorder Using Features Previously Extracted From Structural And Functional Mri. In Proceedings of the 2019 IEEE 16th International Symposium on Biomedical Imaging (ISBI 2019), Venice, Italy, 8–11 April 2019; pp. 1891–1895. [[CrossRef](#)]
62. Wang, W.; Wu, X.; Yuan, X.; Gao, Z. An experiment-based review of low-light image enhancement methods. *IEEE Access* **2020**, *8*, 87884–87917. [[CrossRef](#)]
63. Salem, N.; Malik, H.; Shams, A. Medical image enhancement based on histogram algorithms. *Procedia Comput. Sci.* **2019**, *163*, 300–311. [[CrossRef](#)]
64. Bao, S.; Bermudez, C.; Huo, Y.; Parvathaneni, P.; Rodriguez, W.; Resnick, S.M.; D’Haese, P.F.; McHugo, M.; Heckers, S.; Dawant, B.M. Registration-based image enhancement improves multi-atlas segmentation of the thalamic nuclei and hippocampal subfields. *Magn. Reson. Imaging* **2019**, *59*, 143–152. [[CrossRef](#)]
65. Zhao, C.; Wang, Z.; Li, H.; Wu, X.; Qiao, S.; Sun, J. A new approach for medical image enhancement based on luminance-level modulation and gradient modulation. *Biomed. Signal Process. Control* **2019**, *48*, 189–196. [[CrossRef](#)]
66. Yugander, P.; Tejaswini, C.; Meenakshi, J.; Varma, B.S.; Jagannath, M. MR image enhancement using adaptive weighted mean filtering and homomorphic filtering. *Procedia Comput. Sci.* **2020**, *167*, 677–685. [[CrossRef](#)]
67. Sagheer, S.V.M.; George, S.N. A review on medical image denoising algorithms. *Biomed. Signal Process. Control* **2020**, *61*, 102036. [[CrossRef](#)]
68. Park, W.J.; Schauder, K.B.; Zhang, R.; Benetto, L.; Tadin, D. High internal noise and poor external noise filtering characterize perception in autism spectrum disorder. *Sci. Rep.* **2017**, *7*, 17584. [[CrossRef](#)]
69. Yankowitz, L.D.; Herrington, J.D.; Yerys, B.E.; Pereira, J.A.; Pandey, J.; Schultz, R.T. Evidence against the “normalization” prediction of the early brain overgrowth hypothesis of autism. *Mol. Autism* **2020**, *11*, 1–17. [[CrossRef](#)]
70. Hoeksma, M.R.; Kenemans, J.L.; Kemner, C.; van Engeland, H. Variability in spatial normalization of pediatric and adult brain images. *Clin. Neurophysiol.* **2005**, *116*, 1188–1194. [[CrossRef](#)]
71. Delisle, P.L.; Anctil-Robitaille, B.; Desrosiers, C.; Lombaert, H. Realistic Image Normalization for Multi-Domain Segmentation. *Med. Image Anal.* **2021**, *74*, 102191. [[CrossRef](#)]
72. Ahammed, M.S.; Niu, S.; Ahmed, M.R.; Dong, J.; Gao, X.; Chen, Y. DarkASDNet: Classification of ASD on Functional MRI Using Deep Neural Network. *Front. Neuroinform.* **2021**, *20*. [[CrossRef](#)]
73. Dekhil, O.; Ali, M.; Haweel, R.; Elnakib, Y.; Ghazal, M.; Hajjdiab, H.; Fraiwan, L.; Shalaby, A.; Soliman, A.; Mahmoud, A. A comprehensive framework for differentiating autism spectrum disorder from neurotypicals by fusing structural MRI and resting state functional MRI. In *Seminars in Pediatric Neurology*; Elsevier: Amsterdam, The Netherlands, 2020; Volume 34, p. 100805.
74. Mendes, S.L.; Pinaya, W.H.L.; Pan, P.; Sato, J.R. Estimating Gender and Age from Brain Structural MRI of Children and Adolescents: A 3D Convolutional Neural Network Multitask Learning Model. *Comput. Intell. Neurosci.* **2021**, *2021*, 5550914. [[CrossRef](#)] [[PubMed](#)]
75. Ashburner, J.; Friston, K.J. Voxel-based morphometry—The methods. *Neuroimage* **2000**, *11*, 805–821. [[CrossRef](#)]
76. Haweel, R.; Shalaby, A.; Mahmoud, A.; Seada, N.; Ghoniemy, S.; Ghazal, M.; Casanova, M.F.; Barnes, G.N.; El-Baz, A. A robust DWT-CNN-based CAD system for early diagnosis of autism using task-based fMRI. *Med. Phys.* **2021**, *48*, 2315–2326. [[CrossRef](#)]
77. K, D.; Murthy Oruganti, V.R. A Machine Learning Approach for Diagnosing Neurological Disorders using Longitudinal Resting-State fMRI. In Proceedings of the 2021 11th International Conference on Cloud Computing, Data Science Engineering (Confluence), Noida, India, 28–29 January 2021; pp. 494–499. [[CrossRef](#)]
78. Dekhil, O.; Ali, M.; El-Nakieb, Y.; Shalaby, A.; Soliman, A.; Switala, A.; Mahmoud, A.; Ghazal, M.; Hajjdiab, H.; Casanova, M.F. A personalized autism diagnosis CAD system using a fusion of structural MRI and resting-state functional MRI data. *Front. Psychiatry* **2021**, *10*, 392. [[CrossRef](#)]
79. Yang, X.; Islam, M.S.; Khaled, A.M.A. Functional connectivity magnetic resonance imaging classification of autism spectrum disorder using the multisite ABIDE dataset. In Proceedings of the 2019 IEEE EMBS International Conference on Biomedical Health Informatics (BHI), Chicago, IL, USA, 19–22 May 2019; pp. 1–4. [[CrossRef](#)]
80. Gao, J.; Chen, M.; Li, Y.; Gao, Y.; Li, Y.; Cai, S.; Wang, J. Multisite Autism Spectrum Disorder Classification Using Convolutional Neural Network Classifier and Individual Morphological Brain Networks. *Front. Neurosci.* **2021**, *14*, 1473. [[CrossRef](#)]
81. Squarcina, L.; Nosari, G.; Marin, R.; Castellani, U.; Bellani, M.; Bonivento, C.; Fabbro, F.; Molteni, M.; Brambilla, P. Automatic classification of autism spectrum disorder in children using cortical thickness and support vector machine. *Brain Behav.* **2021**, *11*, e2238. [[CrossRef](#)] [[PubMed](#)]
82. Heinsfeld, A.S.; Franco, A.R.; Craddock, R.C.; Buchweitz, A.; Meneguzzi, F. Identification of autism spectrum disorder using deep learning and the ABIDE dataset. *Neuroimage Clin.* **2018**, *17*, 16–23. [[CrossRef](#)]
83. Alvarez-Jimenez, C.; Munera Garzon, N.; Zuluaga, M.A.; Velasco, N.F.; Romero, E. Autism spectrum disorder characterization in children by capturing local regional brain changes in MRI. *Med. Phys.* **2020**, *47*, 119–131. [[CrossRef](#)] [[PubMed](#)]

84. Madine, M.; Rekek, I.; Werghe, N. Diagnosing Autism Using T1-W MRI With Multi-Kernel Learning and Hypergraph Neural Network. In Proceedings of the 2020 IEEE International Conference on Image Processing (ICIP), Virtual, 25–28 September 2020; pp. 438–442. [CrossRef]
85. Wang, C.; Xiao, Z.; Wu, J. Functional connectivity-based classification of autism and control using SVM-RFECV on rs-fMRI data. *Phys. Medica* **2019**, *65*, 99–105. [CrossRef]
86. Fu, Y.; Zhang, J.; Li, Y.; Shi, J.; Zou, Y.; Guo, H.; Li, Y.; Yao, Z.; Wang, Y.; Hu, B. A novel pipeline leveraging surface-based features of small subcortical structures to classify individuals with autism spectrum disorder. *Prog. Neuro-Psychopharmacol. Biol. Psychiatry* **2021**, *104*, 109989. [CrossRef] [PubMed]
87. Shi, C.; Zhang, J.; Wu, X. An fMRI feature selection method based on a minimum spanning tree for identifying patients with autism. *Symmetry* **2020**, *12*, 1995. [CrossRef]
88. You, Y.; Liu, H.; Zhang, S.; Shao, L. Classification of Autism Based on fMRI Data with Feature-Fused Convolutional Neural Network. In *Cyberspace Data and Intelligence, and Cyber-Living, Syndrome, and Health*; Springer: Berlin/Heidelberg, Germany, 2020; pp. 77–88.
89. Byeon, K.; Kwon, J.; Hong, J.; Park, H. Artificial Neural Network Inspired by Neuroimaging Connectivity: Application in Autism Spectrum Disorder. In Proceedings of the 2020 IEEE International Conference on Big Data and Smart Computing (BigComp), Busan, Korea, 19–22 February 2020; pp. 575–578. [CrossRef]
90. Soeiro, J.; Dias, L.; Silva, A.; Tomé, A. Radiomic Analysis of Brain MRI: A Case Study in Autism Spectrum Disorder. Available online: [https://reepad2021.uevora.pt/wp-content/uploads/2020/10/RECPAD\\_2020\\_paper\\_9.pdf](https://reepad2021.uevora.pt/wp-content/uploads/2020/10/RECPAD_2020_paper_9.pdf) (accessed on 23 August 2021).
91. Ma, X.; Wang, X.H.; Li, L. Identifying individuals with autism spectrum disorder based on the principal components of whole-brain phase synchrony. *Neurosci. Lett.* **2021**, *742*, 135519. [CrossRef]
92. Husna, R.N.S.; Syafeeza, A.; Hamid, N.A.; Wong, Y.; Raihan, R.A. Functional Magnetic Resonance Imaging for Autism Spectrum Disorder Detection Using Deep Learning. *J. Teknol.* **2021**, *83*, 45–52. [CrossRef]
93. Sherkatghanad, Z.; Akhondzadeh, M.; Salari, S.; Zomorodi-Moghadam, M.; Abdar, M.; Acharya, U.R.; Khosrowabadi, R.; Salari, V. Automated detection of autism spectrum disorder using a convolutional neural network. *Front. Neurosci.* **2020**, *13*, 1325. [CrossRef] [PubMed]
94. Raki, M.; Cabezas, M.; Kushibar, K.; Oliver, A.; Llad, X. Improving the detection of autism spectrum disorder by combining structural and functional MRI information. *Neuroimage Clin.* **2020**, *25*, 102181. [CrossRef] [PubMed]
95. Thomas, R.M.; Gallo, S.; Cerliani, L.; Zhutovsky, P.; El-Gazzar, A.; van Wingen, G. Classifying autism spectrum disorder using the temporal statistics of resting-state functional MRI data with 3D convolutional neural networks. *Front. Psychiatry* **2020**, *11*, 440. [CrossRef]
96. Shrivastava, S.; Mishra, U.; Singh, N.; Chandra, A.; Verma, S. Control or Autism—Classification using Convolutional Neural Networks on Functional MRI. In Proceedings of the 2020 11th International Conference on Computing, Communication and Networking Technologies (ICCCNT), Kharagapur, India, 1–3 July 2020; pp. 1–6. [CrossRef]
97. Liu, J.; Sheng, Y.; Lan, W.; Guo, R.; Wang, Y.; Wang, J. Improved ASD classification using dynamic functional connectivity and multi-task feature selection. *Pattern Recognit. Lett.* **2020**, *138*, 82–87. [CrossRef]
98. Zhang, Z.; Zheng, W. The Discriminative Power of White Matter Microstructures for Autism Diagnosis. *IFAC-PapersOnLine* **2020**, *53*, 446–451. [CrossRef]
99. Bayram, M.A.; İlyas, Ö.; Temurtaş, F. Deep Learning Methods for Autism Spectrum Disorder Diagnosis Based on fMRI Images. *Sak. Univ. J. Comput. Inf. Sci.* **2021**, *4*, 142–155.
100. Almuqhim, F.; Saeed, F. ASD-SAENet: A Sparse Autoencoder, and Deep-Neural Network Model for Detecting Autism Spectrum Disorder (ASD) Using fMRI Data. *Front. Comput. Neurosci.* **2021**, *15*, 27. [CrossRef]
101. Ali, M.T.; Elnakieb, Y.A.; Shalaby, A.; Mahmoud, A.; Switala, A.; Ghazal, M.; Khelifi, A.; Fraiwan, L.; Barnes, G.; El-Baz, A. Autism Classification Using SMRI: A Recursive Features Selection Based on Sampling from Multi-Level High Dimensional Spaces. In Proceedings of the 2021 IEEE 18th International Symposium on Biomedical Imaging (ISBI), Virtual, 13–16 April 2021; pp. 267–270. [CrossRef]
102. Lu, P.; Li, X.; Hu, L.; Lu, L. Integrating genomic and resting State fMRI for efficient autism spectrum disorder classification. In *Multimedia Tools and Applications*; Springer: Berlin/Heidelberg, Germany, 2021; pp. 1–12.
103. Chaitra, N.; Vijaya, P.; Deshpande, G. Diagnostic prediction of autism spectrum disorder using complex network measures in a machine learning framework. *Biomed. Signal Process. Control* **2020**, *62*, 102099. [CrossRef]
104. Haweel, R.; Shalaby, A.; Mahmoud, A.; Ghazal, M.; Seada, N.; Ghoniemy, S.; Barnes, G.; El-Baz, A. A Novel Dwt-Based Discriminant Features Extraction From Task-Based Fmri: An Asd Diagnosis Study Using Cnn. In Proceedings of the 2021 IEEE 18th International Symposium on Biomedical Imaging (ISBI), Kolkata, India, 28–31 March 2021; pp. 196–199. [CrossRef]
105. Al-Hiyali, M.I.; Yahya, N.; Faye, I.; Khan, Z.; Alsaih, K. Classification of BOLD FMRI Signals using Wavelet Transform and Transfer Learning for Detection of Autism Spectrum Disorder. In Proceedings of the 2020 IEEE-EMBS Conference on Biomedical Engineering and Sciences (IECBES), Langkawi, Malaysia, 1–3 March 2021; pp. 94–98. [CrossRef]
106. Li, Z. Segmentation and Recognition of MRI Images of the Brain. Ph.D. Thesis, Jilin University, Changchun, China, 2020.
107. Yang, X.; Zhao, X.; Tjio, G.; Chen, C.; Wang, L.; Wen, B.; Su, Y. Openc—An open Benchmark data set for Corpus Callosum Segmentation and Evaluation. In Proceedings of the 2020 IEEE International Conference on Image Processing (ICIP), Virtual, 25–28 October 2020; pp. 3020–3024.

108. Pieper, S.; Halle, M.; Kikinis, R. 3D Slicer. In Proceedings of the 2004 2nd IEEE International Symposium on Biomedical imaging: Nano to Macro (IEEE Cat No. 04EX821), Arlington, VA, USA, 18 April 2004; pp. 632–635.
109. Dolz, J.; Desrosiers, C.; Ayed, I.B. 3D fully convolutional networks for subcortical segmentation in MRI: A large-scale study. *NeuroImage* **2018**, *170*, 456–470. [[CrossRef](#)]
110. Fischl, B. FreeSurfer. *Neuroimage* **2012**, *62*, 774–781. [[CrossRef](#)]
111. Hegarty, J.P.; II, L.C.L.; Raman, M.M.; Hallmayer, J.F.; Cleveland, S.C.; Wolke, O.N.; Phillips, J.M.; Reiss, A.L.; Hardan, A.Y. Genetic and environmental influences on corticostriatal circuits in twins with autism. *J. Psychiatry Neurosci. JPN* **2020**, *45*, 188. [[CrossRef](#)]
112. Wu, C.; Zheng, H.; Wu, H.; Tang, Y.; Li, F.; Wang, D. Age-related Brain Morphological Alteration of Medication-naive Boys With High Functioning Autism. *Acad. Radiol.* **2020**. [[CrossRef](#)]
113. Kumar, G.; Bhatia, P.K. A Detailed Review of Feature Extraction in Image Processing Systems. In Proceedings of the 2014 Fourth International Conference on Advanced Computing Communication Technologies, Rohtak, India, 8–9 February 2014; pp. 5–12. [[CrossRef](#)]
114. Subbaraju, V.; Suresh, M.B.; Sundaram, S.; Narasimhan, S. Identifying differences in brain activities and an accurate detection of autism spectrum disorder using resting state functional-magnetic resonance imaging: A spatial filtering approach. *Med. Image Anal.* **2017**, *35*, 375–389. [[CrossRef](#)]
115. El-Gazzar, A.; Quaak, M.; Cerliani, L.; Bloem, P.; van Wingen, G.; Thomas, R.M. A hybrid 3dcnn and 3dc-lstm based model for 4d spatio-temporal fMRI data: An abide autism classification study. In *OR 2.0 Context-Aware Operating Theaters and Machine Learning in Clinical Neuroimaging*; Springer: Berlin/Heidelberg, Germany, 2019; pp. 95–102.
116. Kou, Q. Research on Image Texture Feature Extraction Method Based on Principal Curvature. Ph.D. Thesis, China University of Mining and Technology (Jiangsu), Xuzhou, China, 2019.
117. Zebari, R.; Abdulazeez, A.; Zeebaree, D.; Zebari, D.; Saeed, J. A comprehensive review of dimensionality reduction techniques for feature selection and feature extraction. *J. Appl. Sci. Technol. Trends* **2020**, *1*, 56–70. [[CrossRef](#)]
118. Urbanowicz, R.J.; Meeker, M.; La Cava, W.; Olson, R.S.; Moore, J.H. Relief-based feature selection: Introduction and review. *J. Biomed. Inform.* **2018**, *85*, 189–203. [[CrossRef](#)] [[PubMed](#)]
119. Chen, C.W.; Tsai, Y.H.; Chang, F.R.; Lin, W.C. Ensemble feature selection in medical datasets: Combining filter, wrapper, and embedded feature selection results. *Expert Syst.* **2020**, *37*, e12553. [[CrossRef](#)]
120. Bommert, A.; Sun, X.; Bischl, B.; Rahnenführer, J.; Lang, M. Benchmark for filter methods for feature selection in high-dimensional classification data. *Comput. Stat. Data Anal.* **2020**, *143*, 106839. [[CrossRef](#)]
121. Solorio-Fernández, S.; Carrasco-Ochoa, J.A.; Martínez-Trinidad, J.F. A review of unsupervised feature selection methods. *Artif. Intell. Rev.* **2020**, *53*, 907–948. [[CrossRef](#)]
122. Rahman, M.; Usman, O.L.; Muniyandi, R.C.; Sahran, S.; Mohamed, S.; Razak, R.A. A Review of machine learning methods of feature selection and classification for autism spectrum disorder. *Brain Sci.* **2020**, *10*, 949. [[CrossRef](#)] [[PubMed](#)]
123. Pavithra, V.; Jayalakshmi, V. Review of Feature Selection Techniques for Predicting Diseases. In Proceedings of the 2020 5th International Conference on Communication and Electronics Systems (ICCES), Coimbatore, India, 10–12 June 2020; pp. 1213–1217.
124. Nielsen, A.N.; Barch, D.M.; Petersen, S.E.; Schlaggar, B.L.; Greene, D.J. Machine learning with neuroimaging: Evaluating its applications in psychiatry. *Biol. Psychiatry Cogn. Neurosci. Neuroimaging* **2020**, *5*, 791–798. [[CrossRef](#)]
125. Ronicko, J.F.A.; Thomas, J.; Thangavel, P.; Koneru, V.; Langs, G.; Dauwels, J. Diagnostic classification of autism using resting-state fMRI data improves with full correlation functional brain connectivity compared to partial correlation. *J. Neurosci. Methods* **2020**, *345*, 108884. [[CrossRef](#)]
126. Haweel, R.; Dekhil, O.; Shalaby, A.; Mahmoud, A.; Ghazal, M.; Khalil, A.; Keynton, R.; Barnes, G.; El-Baz, A. A novel framework for grading autism severity using task-based fmri. In Proceedings of the 2020 IEEE 17th International Symposium on Biomedical Imaging (ISBI), Iowa City, IA, USA, 3–7 April 2020; pp. 1404–1407.
127. Mostafa, S.; Tang, L.; Wu, F.X. Diagnosis of autism spectrum disorder based on eigenvalues of brain networks. *IEEE Access* **2019**, *7*, 128474–128486. [[CrossRef](#)]
128. Huang, Z.A.; Zhu, Z.; Yau, C.H.; Tan, K.C. Identifying autism spectrum disorder from resting-state fMRI using deep belief network. *IEEE Trans. Neural Netw. Learn. Syst.* **2020**, *32*, 2847–2861. [[CrossRef](#)]
129. Abdullah, A.A.; Rijal, S.; Dash, S.R. Evaluation on Machine Learning Algorithms for Classification of Autism Spectrum Disorder (ASD). *J. Phys. Conf. Ser.* **2019**, *1372*, 012052. [[CrossRef](#)]
130. Zhuang, J.; Dvornek, N.C.; Zhao, Q.; Li, X.; Ventola, P.; Duncan, J.S. Prediction of treatment outcome for autism from structure of the brain based on sure independence screening. In Proceedings of the 2019 IEEE 16th International Symposium on Biomedical Imaging (ISBI 2019), Venice, Italy, 8–11 April 2019; pp. 404–408.
131. Chen, H.; Duan, X.; Liu, F.; Lu, F.; Ma, X.; Zhang, Y.; Uddin, L.Q.; Chen, H. Multivariate classification of autism spectrum disorder using frequency-specific resting-state functional connectivity—A multi-center study. *Prog. Neuro-Psychopharmacol. Biol. Psychiatry* **2016**, *64*, 1–9. [[CrossRef](#)]
132. Jahedi, A. Novel Random Forest Methods and Algorithms for Autism Spectrum Disorders Research. Ph.D. Thesis, The Claremont Graduate University, Claremont, CA, USA, 2020.

133. Grossard, C.; Dapogny, A.; Cohen, D.; Bernheim, S.; Juillet, E.; Hamel, F.; Hun, S.; Bourgeois, J.; Pellerin, H.; Serret, S. Children with autism spectrum disorder produce more ambiguous and less socially meaningful facial expressions: An experimental study using random forest classifiers. *Mol. Autism* **2020**, *11*, 1–14. [[CrossRef](#)]
134. Amit, Y.; Geman, D. Shape quantization and recognition with randomized trees. *Neural Comput.* **1997**, *9*, 1545–1588. [[CrossRef](#)]
135. Berrar, D. Cross-Validation. In *Encyclopedia of Bioinformatics and Computational Biology*; Academic Press: Waltham, MA, USA, 2019; pp. 542–545.
136. Choi, J.Y. Radiomics and deep learning in clinical imaging: What should we do? *Nucl. Med. Mol. Imaging* **2018**, *52*, 89–90. [[CrossRef](#)] [[PubMed](#)]
137. Aickin, M.; Gensler, H. Adjusting for multiple testing when reporting research results: The Bonferroni vs. Holm methods. *Am. J. Public Health* **1996**, *86*, 726–728. [[CrossRef](#)]
138. Raj, S.; Masood, S. Analysis and detection of autism spectrum disorder using machine learning techniques. *Procedia Comput. Sci.* **2020**, *167*, 994–1004. [[CrossRef](#)]
139. Dominic, N.; Cenggoro, T.W.; Budiarto, A.; Pardamean, B. Transfer learning using inception-ResNet-v2 model to the augmented neuroimages data for autism spectrum disorder classification. *Commun. Math. Biol. Neurosci.* **2021**. Available online: <http://www.scik.org/index.php/cmbn/article/view/5565> (accessed on 23 August 2021).
140. Goldfeld, Z.; Polyanskiy, Y. The information bottleneck problem and its applications in machine learning. *IEEE J. Sel. Areas Inf. Theory* **2020**, *1*, 19–38. [[CrossRef](#)]
141. Mateen, B.A.; Liley, J.; Denniston, A.K.; Holmes, C.C.; Vollmer, S.J. Improving the quality of machine learning in health applications and clinical research. *Nat. Mach. Intell.* **2020**, *2*, 554–556. [[CrossRef](#)]
142. Chen, X.; Wang, X.; Zhang, K.; Zhang, R.; Fung, K.M.; Thai, T.C.; Moore, K.; Mannel, R.S.; Liu, H.; Zheng, B. Recent advances and clinical applications of deep learning in medical image analysis. *arXiv* **2021**, arXiv:2105.13381.
143. Castelvechi, D. Can we open the black box of AI? *Nat. News* **2016**, *538*, 20. [[CrossRef](#)]
144. Fellous, J.M.; Sapiro, G.; Rossi, A.; Mayberg, H.; Ferrante, M. Explainable Artificial Intelligence for Neuroscience: Behavioral Neurostimulation. *Front. Neurosci.* **2019**, *13*, 1346. [[CrossRef](#)] [[PubMed](#)]
145. Ruan, M.; Webster, P.J.; Li, X.; Wang, S. Deep Neural Network Reveals the World of Autism From a First-Person Perspective. *Autism Res.* **2021**, *14*, 333–342. [[CrossRef](#)] [[PubMed](#)]
146. Chaddad, A.; Hassan, L.; Desrosiers, C. Deep Radiomic Analysis for Predicting Coronavirus Disease 2019 in Computerized Tomography and X-ray Images. *IEEE Trans. Neural Netw. Learn. Syst.* **2021**, 1–9. [[CrossRef](#)]
147. Zeiler, M.D.; Taylor, G.W.; Fergus, R. Adaptive deconvolutional networks for mid and high level feature learning. In Proceedings of the 2011 International Conference on Computer Vision, Barcelona, Spain, 6–13 November 2011; pp. 2018–2025.
148. Zhang, Q.; Wu, Y.N.; Zhu, S.C. Interpretable convolutional neural networks. In Proceedings of the IEEE Conference on Computer Vision and Pattern Recognition, Salt Lake City, UT, USA, 18–23 June 2018; pp. 8827–8836.
149. Chaddad, A.; Toews, M.; Desrosiers, C.; Niazi, T. Deep Radiomic Analysis Based on Modeling Information Flow in Convolutional Neural Networks. *IEEE Access* **2019**, *7*, 97242–97252. [[CrossRef](#)]
150. Mayor-Torres, J.M.; Ravanelli, M.; Medina-DeVilliers, S.E.; Lerner, M.D.; Riccardi, G. Interpretable SincNet-based Deep Learning for Emotion Recognition from EEG brain activity. *arXiv* **2021**, arXiv:2107.10790.
151. Biswas, M.; Kaiser, M.S.; Mahmud, M.; Al Mamun, S.; Hossain, M.; Rahman, M.A. An XAI Based Autism Detection: The Context Behind the Detection. In Proceedings of the International Conference on Brain Informatics, Virtual, 17–19 September 2021; pp. 448–459.
152. Lundberg, S.M.; Lee, S.I. A unified approach to interpreting model predictions. In Proceedings of the 31st International Conference on Neural Information Processing Systems, Long Beach, CA, USA, 4–9 December 2017; pp. 4768–4777.
153. Tjoa, E.; Guan, C. A Survey on Explainable Artificial Intelligence (XAI): Toward Medical XAI. *IEEE Trans. Neural Netw. Learn. Syst.* **2020**, 1–21. [[CrossRef](#)]
154. Parekh, V.S.; Jacobs, M.A. Radiomic Synthesis Using Deep Convolutional Neural Networks. In Proceedings of the 2019 IEEE 16th International Symposium on Biomedical Imaging (ISBI 2019), Venice, Italy, 8–11 April 2019; pp. 1114–1117. [[CrossRef](#)]
155. Cui, L.B.; Xu, X.; Cao, F. Building the precision medicine for mental disorders via radiomics/machine learning and neuroimaging. *Front. Neurosci.* **2021**, *15*, 650. [[CrossRef](#)] [[PubMed](#)]
156. Thabtah, F. Machine learning in autistic spectrum disorder behavioral research: A review and ways forward. *Inform. Health Soc. Care* **2019**, *44*, 278–297. [[CrossRef](#)]
157. de Belen, R.A.J.; Bednarz, T.; Sowmya, A.; Del Favero, D. Computer vision in autism spectrum disorder research: A systematic review of published studies from 2009 to 2019. *Transl. Psychiatry* **2020**, *10*, 1–20. [[CrossRef](#)]